F_y^* and η^* are the bathystropic transport and bathystropic storm tide respectively. In other words, we write

$$\frac{\partial F_y^*}{\partial t} = \frac{\tau_y}{\rho} \tag{17}$$

$$-gh\frac{\partial \eta^*}{\partial x} + f F_y^* + \frac{\tau_x}{\rho} = 0 . \tag{18}$$

From (14), (16), and the definition above, we can write

$$\partial F_x' = -gh\frac{\partial \eta'}{\partial x} + f F_y' \tag{19}$$

$$\partial F_y' = -f F_x' \tag{20}$$

$$\frac{\partial \eta'}{\partial t} = -\frac{\partial F_x'}{\partial x} - \frac{\partial \eta^*}{\partial t} . \tag{21}$$

Equations (17) and (18) are interesting. They show that for this one-dimensional problem we can compute the bathystrophic flux, F_y^*, and the storm tide, η^*, for all time and then use the time history of η^* in (19) to (21) to compute F_x', F_y', and η'.

We can solve a particular problem for F_x', F_y', and η', and we have shown that η^* soon becomes (and stays) much larger than η'. This problem is worked for a straight coast with a linear bottom profile of slope 1/1,000. We assume that the origin is at the shore and that no significant changes in η occur farther out than $x = -45 \times 10^4$ ft.

The computation can be carried out by the method of characteristics as described by Freeman (1951). The basic computing formulae found by applying this method to (19) and (20) are that the conditions

$$\frac{dF_x'}{dt} \pm \sqrt{gh}\frac{d\eta'}{dt} = f F_x' \mp \sqrt{gh}\frac{d\eta^*}{dt} \tag{22}$$

hold along the lines with slope

$$\frac{dx}{dt} = \pm\sqrt{gh} . \tag{23}$$

We assume the bathystrophic flux F_y^* is such that

$$\frac{\partial \eta^*}{\partial t} = (1.85 \times 10^{-10} x + 8.3 \times 10^{-5}) \text{ kts.}$$

Starting with the water absolutely level and computing for two hours with $\partial\eta^*/\partial t$ as given above, we compute the time history at the shore, which is illustrated in Fig. 5.

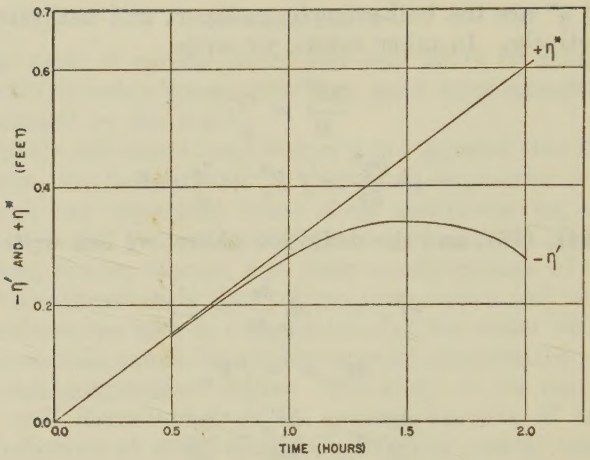

Figure 5. The bathystrophic storm tide, η^*, compared with the deviation from the bathystrophic storm tide η' as computed by the method of characteristics.

Note that in this time η^* becomes 0.59 feet at the shore and η' becomes —.30 feet. η^* is still increasing at the initial rate, but $|\eta'|$ is now decreasing. The plot of η' and η^* vs. time at other values of x show a similar behavior.

This study indicates that η' stays near the values reached after two hours while η^* increases indefinitely. Thus η' does not become significant, and F_x' and F_y' remain insignificant compared to $F_y{}^*$. Thus our first assumption is justified in this model which would have allowed it to be violated.

REFERENCES

J. C. Freeman

1951. The solution of nonlinear meteorological problems by the method of characteristics, in Compendium of Meteorology. Amer. meteorol. Soc., Boston, 1951: 421–433.

J. C. Freeman, Jr. and Ledolph Baer

1956. Graphical computation of storm tides. Rep. to U. S. Weather Bureau under Contract No. Cwb–8687. Unpublished.

1957. The method of wave derivatives. Trans. Amer. geophys. Un., *38* (4): 483–494.

R. K. Linsley, M. A. Kohler, and J. L. H. Paulhus

1949. Applied Hydrology. McGraw-Hill, New York. 689 pp.

W. H. Munk, Frank Snodgrass and George Carrier

1956. Edge waves on the continental shelf. Science, *123* (3187): 127–132.

ACCELERATION MEASUREMENTS IN THE DEEP OCEAN[1]

By

F. N. SPIESS

University of California
Marine Physical Laboratory of the
Scripps Institution of Oceanography

ABSTRACT

The study of surface waves in the deep ocean can be carried out effectively by using a new technique: measurement of accelerations of a small water mass well below the surface. Instrumentation for carrying out such measurements is described in detail, including a special accelerometer, neutrally buoyant case, long lightweight slack wire, and data-recording equipment. Some initial results achieved with this equipment are shown and the possibility of broader applications of this technique for wave and gravity measurements at sea are discussed briefly.

INTRODUCTION

A major obstacle to the study of waves in the deep ocean is the difficulty in obtaining adequate data concerning the actual motion of the sea surface. This difficulty stems primarily from the lack of an adequate reference level against which to compare the position of any particular small mass of water, either on or below the surface. Over some frequency ranges it is possible, because of the rather large surface amplitudes and rapid attenuation of disturbance with depth, to use a wave pole (Upham, 1955) or other device to determine the motion of the surface relative to the somewhat more immobile subsurface water. This method becomes unsatisfactory for periods greater than about 10 seconds since the vertical attenuation distance is large enough to dictate inconveniently long devices or large correction factors.

An alternative is to measure the acceleration of the water mass rather than the displacement. In this case, the reference used is the force of gravity, which is conveniently available everywhere. Some difficulties arise, however, particularly if the measurement

[1] This paper represents results of research carried out by the University of California under Contract NObsr-72512, NE-120221-4-5-6 with the Bureau of Ships, Navy Department. Contribution from the Scripps Institution of Oceanography, New Series, No. 941.

is carried out at the surface of the water (Tucker, 1955). In the first place, the motion of the vehicle carrying the accelerometer becomes rather complex, including rotational effects which are associated not with the motion of the water at any one place but with its integrated effect over the entire body of the vehicle. A second and perhaps more fundamental problem arises from the fact that the higher frequencies are accentuated relative to the lows in a very pronounced fashion—in fact, as the square of the frequency. This is particularly awkward, for instance, if one is primarily interested in the low frequency end of the surface wave spectrum.

The method to be described below in detail minimizes the shortcomings of the acceleration measuring approach by placing the sensing element in a small case well down in the water, remote from the ship. In this way the motion of the meter is quite similar to that of a small particle of water; at the same time the rapid attenuation of the short period waves with depth compensates for the accentuation of the high frequencies.

Basically the measurements are carried out by operating an accelerometer in a nearly neutrally-buoyant small case connected to the operating ship by a long, slack, flexible wire. This technique has been used in underwater acoustics by many groups to obtain quiet operation of hydrophones at sea in seismic refraction and ambient noise measurements.

The principal components are the pressure proof case, the slack wire and winch, a depth measuring system, and the accelerometer itself. The important characteristics of each of these are described in the following sections: Accelerometer and Other Components. The section on Operation describes the system at sea, and the Discussion considers future developments and uses which can be made of this technique.

ACCELEROMETER

The accelerometer as conceived dictated the following requirements: compactness; an easily built sensing unit and a linear system; measurable response to acceleration changes of about 0.01 cm/sec^2; mechanical resonant frequencies that are high compared with one cycle per second; an output which would be easy to transmit reliably on a wire and which would be easy to average over arbitrarily long intervals. The dynamic range would have to be greater than 10 cm/sec^2.

All of these features pointed to a stiff spring with a direct electrical determination of its deflection. The resulting sensing element is

shown in Fig. 1. It consists of a short but broad leaf-spring which is 2 in. long, 1 in. wide and 0.025 in. thick and is machined from a somewhat thicker strip of NiSpan "C", an alloy with low thermal coefficient of Young's modulus. The spring is clamped at one end and loaded at the other with a brass plate, which forms one side of each of three air condensers. The other sides of these condensers are fixed plates of silver on the underside of a glass plate supported above the end of the spring. The shoulders which support the glass plate are machined down far enough to insure that the condenser

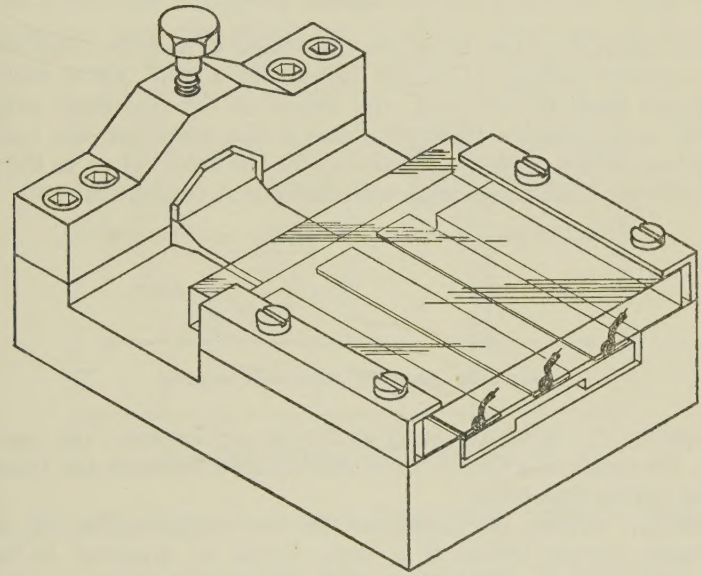

Figure 1. Acceleration sensing element.

gap is only about one-tenth of the total deflection of the spring; thus the condensers short out at accelerations of about 100 cm/sec^2. The mechanical resonance of the spring as loaded with the brass plate lies at 30 cps, which corresponds to a static deflection under gravity of about 0.034 inch.

The shoulders which support the three fixed condenser plates above the deflecting mass were machined down to give an air gap of about 0.002 in. under static conditions. The resulting capacity of each condenser under these conditions is about 125 $\mu\mu f$, which is, as will be seen below, sufficient for the purposes at hand.

In choosing an electrical measuring method for determining the deflection of the spring, it was immediately apparent that requirements

for linearity, ease of transmission and ease of integration could be met by allowing the deflection to control the frequency of an RC phase shift oscillator (Ginzton and Hollingsworth, 1941). In this circuit a phase shift network of the type shown in Fig. 2 is used as the feedback loop in a simple amplifier. If all resistances are equal to R and all condensers have capacity C, then such a network introduces a 180° phase shift at a frequency given by

$$f = \frac{\sqrt{6}}{2\pi RC}. \tag{1}$$

If this network is used to couple the output of a single stage vacuum tube amplifier (which of course introduces a 180° phase shift into the signal) back to its input, any signal at the frequency given by (1) will have positive feedback, and if the amplifier has sufficient gain (about 30 db needed) to make up for the attenuation in the phase shift network, then the system will oscillate at that frequency. Since

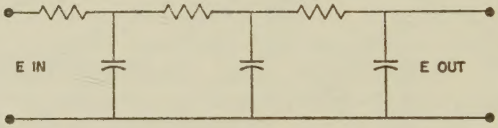

Figure 2. Basic RC phase shift network.

the capacity, C, varies inversely as the air gap between the condenser plates, the result is a direct linear relationship between the frequency and the spring deflection.

Actually, various complications prevent construction of such a completely simple device if a high degree of linearity is needed. Additional vacuum tube stages (cathode followers) must be added to isolate the phase shift network from the amplifying stage so as to achieve minimal effects of driving the network from a nonzero-impedance source and terminating it in a noninfinite impedance. Further, some provision must be made to control the amplitude of the signal, otherwise the amplifier will operate in nonlinear fashion and distort the wave form and output frequency. Care must also be taken in assembling the circuit, since the smallness of the condensers leads to potentially large and variable effects (due to motion of components) from stray capacity between circuit elements and ground. A satisfactory version of the circuit is the one shown in Fig. 3, which has been used in our initial work with this instrument.

Once adequate linearity has been achieved, it is immediately evident that determination of the average deflection of the spring

over any desired averaging time can be achieved in direct fashion by counting cycles of the output with any of the standard frequency counters which are available.

In principle all the quantities necessary for relating the deflection to the frequency are known, but the effects of stray capacity and finite terminating impedances make use of the theoretical values impracticable. Instead, a calibration curve is made conveniently by tilting the instrument to known angles relative to the vertical. Results of such a test on the first instrument built and used showed that the sensitivity was about 0.02 cm/sec^2 per cycle per second change in frequency near the operating oscillator frequency of 9 kc. A

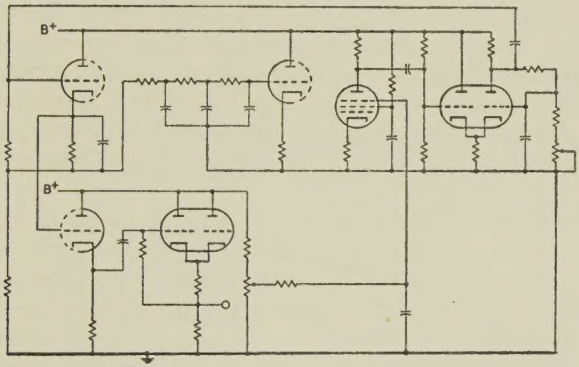

Figure 3. RC phase shift oscillator circuit.

useful dynamic range of at least 2 kc exists, corresponding to 40 cm/sec^2.

Reasonably low frequency drift is required if records of many minutes duration are desired. To achieve this, well regulated power supplies are needed, for both B^+ voltage and filament current. In the present version, power is fed down the lead wire from a current-regulated supply on shipboard. All filaments are operated in series on this power; in addition, current is bled off to a voltage regulating circuit in the pressure proof case and used for B^+ supply. The current regulation is to 1 part in 10^4, while voltage control is to 0.01%.

In addition to power supply control, it is necessary to provide good thermal insulation to minimize frequency drift during the observation period or to operate the instrument in a cold-water environment for a half hour or so before making an observation.

OTHER COMPONENTS

Aside from the accelerometer, the principal components are the case, the slack wire and winch, and the depth-measuring system. The case must protect the equipment from sea pressure and at the same time it must be large enough and light enough to provide adequate buoyancy. The shell shown in Fig. 4 was fabricated from 8 in. aluminum pipe, 61 ST grade, and heat-treated after welding of flanges. Its design-collapse depth is about 1200 ft. Its height of about 30 in. and its weight of 42 lbs results in a net reserve buoyancy of 27 lbs to support the necessary equipment. The two thin strands of wire are led through tight-fitting holes in a rubber sheet which is held and supported between an external plate and the top plate of the container. A hydrostatically operated weight dropper is mounted on the bottom of the case, and the weight attached to this provides negative buoyancy to speed the descent of the case to its desired operating depth. Note that the aluminum cylinder used has a compressibility less than that of water; thus it is stable in its hovering characteristics.

The wire, a critical portion of this system, must be light, watertight, and flexible, yet strong enough to be used to pull in the case; also it must be available in very long lengths. One particular cable, Signal Corps WD1TT Communication Wire, a type of signal corps field wire, is entirely satisfactory. It consists of a twisted pair of wires, each being composed of 4 copper and 3 steel strands, all 30 gage. This wire, being insulated with vinyl and coated with polyethylene, affords completely satisfactory watertight integrity. In water it weighs about 4 lbs per thousand feet, and its breaking tensile strength is greater than 100 lbs. Long continuous runs of 5000- or 6000-foot lengths are easily obtained and are quite satisfactory for this application. The winch, which is shown with the wire on it in Fig. 4, need not be large but it should have two characteristics: it must run freely in order that the wire can be paid out rapidly; and its drive should be designed so that it cannot exert a tension on the wire in excess of the breaking strength.

Two different depth-measuring devices have been used. The first was a dc telemetering system with a bourdon tube sensing element to drive a potentiometer (G. M. Gianini & Co., Pressure Transmitter, Type 46131). The second was an FM telemetering system with a pressure controlled Vibrotron oscillator (Byron Jackson Co., Model 101). Both of these were satisfactory in their absolute accuracy, but the second was preferred because of its smaller hysterisis.

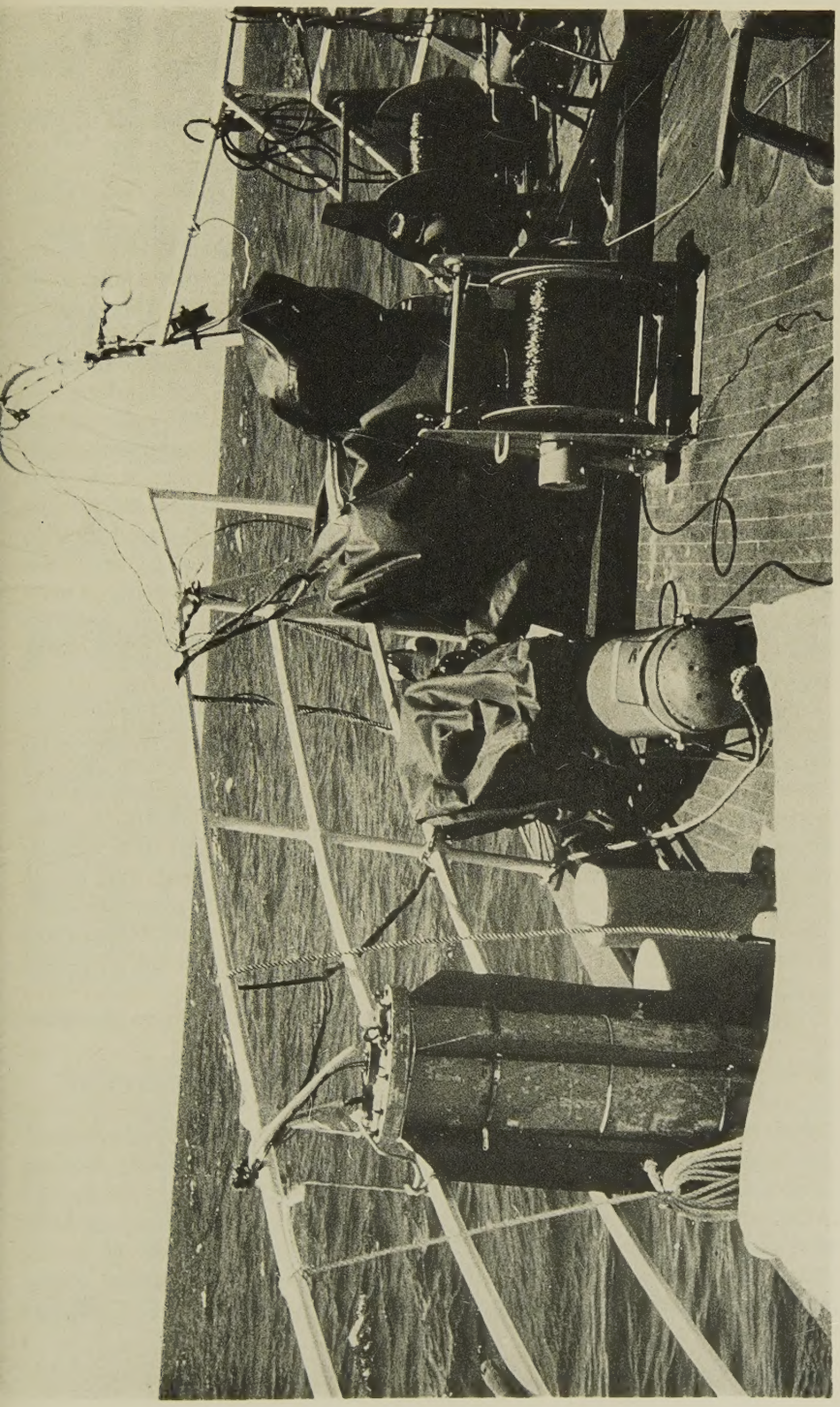

Figure 4. Accelerometer equipment on board R/V STRANGER. The neutrally buoyant case is the vertical cylinder in the left foreground. The winch is at right rear with a spare reel of wire adjacent to it.

OPERATION

In carrying out a measurement, the weight-dropper is set for the desired operating depth and the sinker (usually about 6 lbs) is attached. The case is then put over the side and wire is paid out rapidly. Typically 2000 to 4000 feet of wire would be used, although this varies somewhat with weather conditions. Fish-net floats with about 1 lb buoyancy are attached to the wire at about 200-foot intervals for the first 1000 to 1200 feet; this procedure provides buoyancy to that portion of the wire that is closer to neutral, and it also decreases any tendency for the wire to transmit mechanical jerks along its length from surface to instrument. The instrument case drops initially with a speed of about 2.5 feet per second to the point at which the sinker is released. Almost instantaneously the case stops and then begins to rise very slowly, speeds of less than 0.1 of a foot per second being common. As more wire is paid out, beyond the first 1000 feet, some of the weight of the wire is supported by the case which then begins to sink slowly. Thus the vertical velocity is zero for some section of the run. To date, record lengths of 15 minutes with the case in a 20-foot depth interval near 400 feet have been obtained.

Data have been recorded in two ways. (1) The accelerometer signal is heterodyned down to the 1 kc range and recorded on a conventional tape recorder for eventual analysis upon return to the laboratory; (2) For immediate perusal both depth and acceleration outputs are fed to conventional frequency meters which in turn drive Esterline-Angus recorders. Fig. 5 shows a section of a typical wave acceleration record. This example was taken with the meter at a depth of about 400 feet in water of about 2000 fathoms depth off the coast of southern California. A strong sinusoidal component is evident with a period of about 16 seconds. The maximum variation in acceleration in this record is approximately 0.4 cm/sec^2.

The water acceleration at depth can be converted to wave displace-

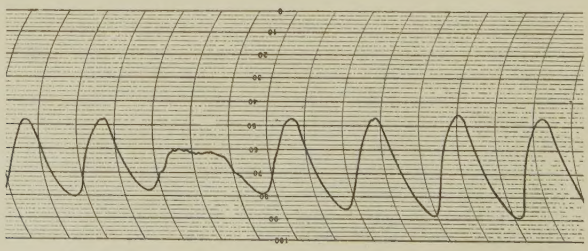

Figure 5. Portion of typical accelerometer record.

ment amplitude at the surface by using the classical theory for deep water waves (Lamb, 1932: Chap. IX), since this is very nearly a single frequency spectrum at 62 cycles per kilosecond. For sinusoidal waves of small amplitude, A, angular frequency, ω, and wave number, k, the theory gives a displacement of

$$\zeta = A\, e^{-kz} \sin (kz - \omega t)$$

at depth z (positive downward). The vertical acceleration would then be

$$\ddot{\zeta} = -\omega^2 A\, e^{-kz} \sin (kz - \omega t).$$

Thus the acceleration amplitude at depth z can be converted to the surface displacement amplitude by

$$A = \ddot{\zeta}_0\, (e^{+kz}/\omega^2).$$

In deep water this becomes:

$$A = \ddot{\zeta}_0\, [e^{+(\omega^2 z/g)}/\omega^2].$$

This expression shows that the conversion factor is large for both very small and very large values of ω and goes through a minimum for depth of observation z_0 at $\omega_0^2 = g/z_0$. The correction factor will be a slowly varying function of frequency in the vicinity of ω_0; thus, if a particular region in the spectrum is of special interest, this can be singled out by operating the meter at $z_0 = g/\omega_0^2$. For waves of 15 seconds period ($\omega = 0.42$ radians per second) this depth is 56 meters.

The analysis above applies specifically to a sinusoidal wave train. However, sophisticated treatment in which more realistic statistical properties of waves are treated leads to the general result that the entire spectrum of the acceleration measured at some depth can be converted to the surface displacement amplitude spectrum by the factor simply derived above.

CONCLUSIONS

The basic principles applied in developing this instrument thus far seem to have been fruitful. The first model was used on the Scripps Institution of Oceanography expedition CHINOOK into the northeastern Pacific during the summer of 1956. Detailed analysis of the data from this cruise is in progress and will be reported at a later date. Preliminary inspection shows that a strong peak exists at a period of 15 to 17 seconds in every record. The surface amplitude of these waves varies but is of the order of a few centimeters to tens of centimeters. The breadth of the spectrum peak is apparently less than

that which can be determined from the record lengths (15 minutes typically) available.

Two major improvements will be incorporated in the instrument prior to its further use. First, two additional accelerometers and a telemetering compass will be installed so that all three acceleration components can be observed simultaneously; from their amplitudes and phase relations, directional information will be obtained. No difficulties are anticipated in this development with the experimental equipment; analysis of the data in terms of an approximation to the directional spectrum will present much more formidable problems. Second, to make the wavemeter more useful, a mechanism for adjusting the buoyancy of the case during an observation must be provided in order to increase appreciably the useful length of the record. Several methods for accomplishing this by remote control within the limits of weight, space and power are being investigated; at least one, utilizing a small high-pressure pump, appears promising.

In addition to its usefulness as a wave measuring device in the open ocean, this same instrument will be tried for measuring gravity at sea from a surface ship. In this case it will be operated at such a depth that the wave amplitudes will be small enough so that the second order horizontal acceleration correction terms can be neglected; this will allow the resultant values to be obtained by simple averaging. Sufficient sensitivity and ease of averaging have already been achieved to reduce uncertainties to near one milligal (0.001 cm/sec^2). The chief obstacle at present is the attainment of the necessary long-term stability; in this connection, development of a suitable temperature regulation system is the problem under consideration.

ACKNOWLEDGMENTS

The development of this instrument has been aided considerably by discussions with Dr. V. C. Anderson and by encouragement from Dr. L. N. Liebermann. Actual construction of the electronic equipment was carried out by Mr. M. McGehee. Mr. J. Joy, who assisted in its operation on the CHINOOK expedition, analyzed the resulting records. We are indebted also to the Hudson Laboratories, Columbia University, which provided the pressure proof case and hydrostatic weight dropper.

REFERENCES

Ginzton, E. L. and L. M. Hollingsworth
1941. Phase-shift oscillators. Proc. Inst. Radio Engrs. N. Y., *29:* 43.
Lamb, Horace
1932. Hydrodynamics. Cambridge Univ. Press. 738 pp.
Tucker, M. J.
1955. A shipborne wave recorder. Proc. 1st Conf. Coast. Engng. Inst., pp. 112–118.
Upham, S. H.
1955. Electric wave staff (Hydrographic Office Model Mark I). Rep. U. S. hydrogr. Off., TR-9 (Unclass.): 1–17.

A NOTE ON THE DYNAMIC BALANCE IN ESTUARINE CIRCULATION

By

R. W. STEWART

Institute of Oceanography, University of British Columbia

ABSTRACT

Because of the large tidal velocities and small dimensions of estuaries, it is not justified to ignore the effects of the curvature of flow when computing the dynamic balance of the current system.

Pritchard (1956), in an analysis of oceanographic data in the James River, has found that the observed lateral gradient of pressure is not exactly balanced by the Coriolis force, as calculated from the observed mean flow. He ascribes the residual force to the gradient of a lateral Reynolds shear stress, and with this assumption he is able to calculate the stress. Pritchard and Kent (1956) then observed that the stress so calculated was, after minor modifications in the assumptions, nearly proportional to the calculated downstream Reynolds shear stress; further, they noted that the constant of proportionality was virtually the same as that obtained by Fleagle and Badgley (1952) in an atmospheric study.

The existence of a lateral Reynolds shear stress in the circumstances noted is not *a priori* likely, and it is the object of this note to offer an alternative interpretation of the data.

We use the notation of Pritchard (1956), hereafter referred to as (I), and of Pritchard and Kent (1956), hereafter referred to as (II), except that we use the tensor summation convention for compactness.

We choose left-handed Cartesian co-ordinates x_i such that: x_1 is directed seaward along the axis of the estuary; x_2 is directed downward; x_3 is directed across the estuary.

Following (I), the instantaneous velocity component v_i in the positive x_i direction is divided into three parts, which are assumed uncorrelated.

Thus:

$$v_i = \bar{v}_i + U_i + v_i', \tag{1}$$

where $\bar{v}_i$ is the Eulerian mean velocity taken over one or more tidal

cycles, U_i is the tidal contribution, and v_i' is the random (turbulent) contribution.

The equation of motion in the x_3 direction is given [I(4)] by:

$$\frac{\partial v_3}{\partial t} + v_j \frac{\partial v_3}{\partial x_j} = -\alpha \frac{\partial p}{\partial x_3} + f v_1 + \alpha \frac{\partial p'_{3j}}{\partial x_j} , \tag{2}$$

where α is the specific volume, f is the Coriolis parameter, and p'_{ij} is a viscous stress.

The viscous stresses are normally important only very close to boundaries and will hereafter be neglected.

If we now substitute (1) in (2) and average over one or more tidal cycles, we obtain, in the steady state:

$$\frac{\partial \bar{v}_j \bar{v}_3}{\partial x_j} + < \frac{\partial U_j U_3}{\partial x_j} > = - < \alpha \frac{\partial p}{\partial x_3} > + f\bar{v}_1 - < \frac{\partial v'_j v'_3}{\partial x_j} > , \tag{3}$$

where the symbol $< \ >$ means averaging as specified and where use has been made of the condition of incompressibility. The x_1 direction was so chosen that $\bar{v}_3 = U_3 = 0$, and if we assume

$$\bar{v}_3 \equiv U_3 \equiv 0 , \tag{4}$$

then we get

$$0 = - < \alpha \frac{\partial p}{\partial x_3} > + f\bar{v}_1 - < \frac{\partial v'_j v'_3}{\partial x_j} > . \tag{5}$$

It is probable (I) that $< \frac{\partial v'_1 v'_3}{\partial x_1} >$ and $< \frac{\partial v'_3 v'_3}{\partial x_3} >$ are very small, so (5) becomes

$$< \frac{\partial v'_2 v'_3}{\partial x_2} > = f\bar{v}_1 - < \alpha \frac{\partial p}{\partial x_3} > . \tag{6}$$

Since $f\bar{v}_1$ and $< \alpha \frac{\partial p}{\partial x_3} >$ may be measured except for a constant, a useful equation describing some aspects of the flow is thus obtained. In (I) an assumption is made regarding the value of the unknown constant, and $<v'_2 \, v'_3>$ is calculated by numerical integration. In (II) an assumption is made which relates the Reynolds stress[1] $<v'_2 \, v'_3>$ to the calculated values of $<v'_1 \, v'_2>$, making possible the calculation of $\bar{v}_1$ from equation (6).

[1] Except for a density term. Strictly, the Reynolds stress is $<\rho \, v'_i \, v'_j>$.

The relation between $<v_1' v_2'>$ and $<v_2' v_3'>$ is taken from some observations of Fleagle and Badgley (1952).[2]

The existence of a finite value for the Reynolds stress $<v_2' v_3'>$ as found in (I) and (II) is surprising. It requires that the turbulent intensity in one direction at 45° to x_2 and x_3 should be greater than that in the other diagonal direction. There seems to be no mechanism present which would cause and maintain this asymmetry. In the circumstances it seems profitable to suspect the accuracy of eq. (4) and therefore of eq. (5) and to re-examine eq. (3).

If the channel is curved and not perfectly straight, then, although $\bar{v}_3 = U_3 = 0$, it is *not* correct to put $\frac{\bar{v}_j \bar{v}_3}{\partial x_j}$ and $\frac{\partial U_j U_3}{\partial x_j} = 0$. It is likely that both $\bar{v}_2$ and U_2 are very small. If we accept the argument that $<v_2' v_3'>$ is also small because of considerations of symmetry, then (3) may be written

$$\frac{\partial}{\partial x_1}\left\{\bar{v}_1\bar{v}_3 + < U_1 U_3 >\right\} = - < \alpha \frac{\partial p}{\partial x_3} > + f\bar{v}_1 \,. \tag{7}$$

The right-hand side of (7) has been calculated for a station in the James River (I, Table III) and the figures show a monotonic variation from $-\ 6{\cdot}31 \times 10^{-6}\ MS^{-2}$ at the surface to $+\ 7{\cdot}32 \times 10^{-6}\ MS^{-2}$ near the bottom, although some of the assumptions used in the derivation are rather arbitrary and a constant of not too large magnitude could be added to each. Because of slightly different assumptions, somewhat different values for these figures are obtained in (II) from those in (I). It is extremely unlikely that the true values lie outside the range $(-7\pm2) \times 10^{-6}\ MS^{-2}$ at the surface and $(+7\pm2) \times 10^{-6}\ MS^{-2}$ near the bottom.

Now, if the radius of curvature of the flow is R, then, in the vicinity of the station where $\bar{v}_3 = U_3 = 0$, we have

$$\frac{\partial \bar{v}_3}{\partial x_1} = \frac{\bar{v}_1}{R}, \tag{8}$$

$$\frac{\partial U_3}{\partial x_1} = \frac{U_1}{R} \,.$$

[2] It is not the purpose of this communication to criticize this work in detail. Suffice it to note that there are several serious objections to the analysis of Fleagle and Badgley, the most important of which is that they have used a Lagrangian average to compute the Reynolds stress. The latter is a strictly Eulerian concept, and therefore their results are of doubtful significance.

Substituting in (7) we find that at the surface

$$R_S \sim -1.4 \times 10^5 M^{-1} S^{-2} (\overline{v}_1^2 + \langle U_i^2 \rangle)_S \tag{9}$$

and near the bottom

$$R_B \sim 1.4 \times 10^5 M^{-1} S^{-2} (\overline{v}_1^2 + \langle U_1^2 \rangle)_B . \tag{10}$$

The particular station in the James River for which the calculations have been carried out is not identified in (I), but by reference to (II) it is fairly clear that both (I) and (II) deal with St. J-17, for which Pritchard and Kent (1953) have published detailed oceanographic

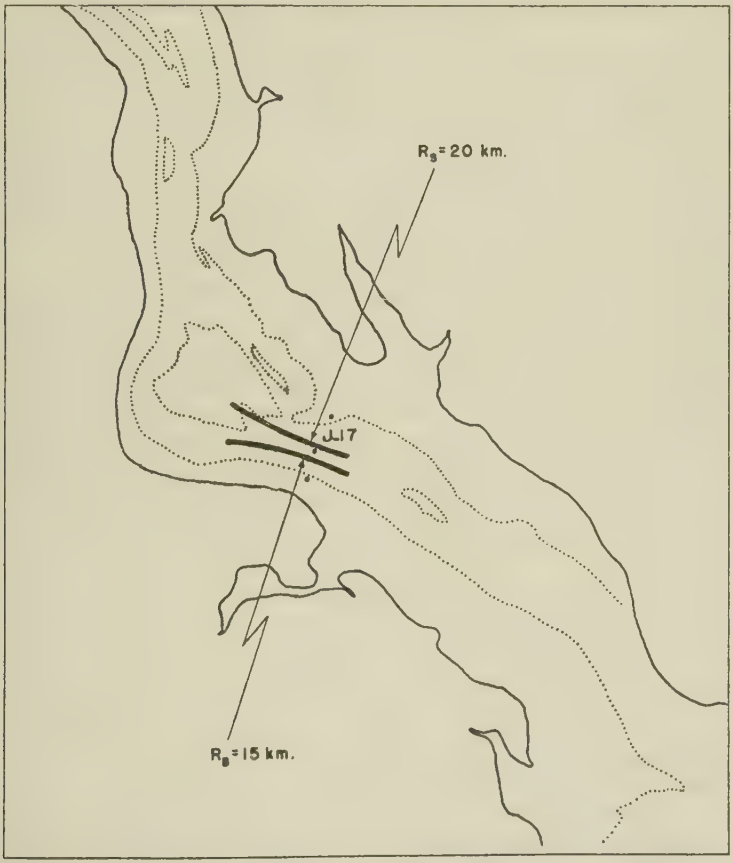

Figure 1. James River in the vicinity of St. J-17, showing the curvature of flow required to account for the observed difference between pressure gradient and Coriolis force. The 10-foot contour is shown dotted.

data. It is observed (Pritchard and Kent, 1953: figs. 2, 3) that $\bar{v}_1$ is about $0.13MS^{-1}$ at the surface and $-0.10MS^{-1}$ at the bottom. The average value of $|U_1|$ appears to be about $0.32MS^{-1}$ at the surface and $0.29MS^{-1}$ near the bottom. If the time variation of U_1 were sinusoidal, this would give:

$$<U_1^2>_S = 0.13\ M^2S^{-2}$$

$$<U_1^2>_B = 0.10\ M^2S^{-2}\ .$$

Substituting these values in (9) and (10) we find that

$$R_S \sim -\ 20\ KM\ , \tag{11}$$

$$R_B \sim 15\ KM\ . \tag{12}$$

These values should be accurate within plus or minus about 30%. In a geographical feature of the dimensions of the James River, flow in a curve of radius of the order of 15–20 *KM* is far from out of the question. Arcs with these radii are shown in Fig. 1, which is a sketch of the portion of the James River near St. J-17. It seems eminently reasonable to suppose that the difference between the pressure gradient and the Coriolis force is largely due to the centrifugal force in curved flow, not to a lateral shearing stress.

It would be unwise to overstate the case. If, as seems likely, the curvature of the flow importantly affects the terms under consideration, then the fact that this curvature varies with depth destroys the symmetry argument originally invoked to reject the lateral shearing stress hypothesis. In this case some lateral stress may well exist. What remains clear is that it is not justified to ignore the effects of curvature in the flow, as has been done in (I) and (II). It is worth noting that the effect is due almost entirely to the fluctuating tidal currents, which produce an influence an order of magnitude greater than does the mean flow.

REFERENCES

Fleagle, R. G. and F. I. Badgley.

1952. Atmospheric turbulence study. Occ. Rep. Dept. Meteorol. Climatol. Univ. of Washington, No. 2: 47 pp.

Pritchard, D. W.

1956. The dynamic structure of a coastal plain estuary. J. Mar. Res., *15* (1): 33–42. Referred to in the Stewart paper as (I).

Pritchard, D. W. and R. E. Kent.

1953. The reduction and analysis of data from the James River operation Oyster Spat. Tech. Rep. Chesapeake Bay Inst. VI, Ref. 53–12: 92 pp.

1956. A method for determining mean longitudinal velocities in a coastal plain estuary. J. Mar. Res., *15* (1): 81–91. Referred to in the Stewart paper as (II).

COMMENT BY DONALD W. PRITCHARD

As an author of the papers discussed by Dr. Stewart and in my capacity as an editor of this JOURNAL, I was asked to review this manuscript prior to publication. I find Dr. Stewart's brief discussion of great interest and consider it to be of considerable importance in the possible significance of curvature in dealing with estuarine circulation. I would like to point out that in the papers discussed by Dr. Stewart it was not my intent to indicate that I considered the lateral velocities precisely zero but rather that the lateral field acceleration terms were negligible. I do believe that there does exist a lateral component to the velocity field which could provide the necessary strain corresponding to the lateral Reynolds stress term. However, in view of this work by Dr. Stewart, it now appears unlikely that my previous treatment adequately evaluates this lateral Reynolds stress term.

A THEORY OF UPWELLING OF LARGE HORIZONTAL EXTENT[1]

By

KOZO YOSHIDA AND HAN-LEE MAO

ABSTRACT

Based on certain hypotheses, vertical motion in the upper layers is found to be related to the poleward transport in the lower layers. Upwelling off the California coast, based on recent data, is examined; the theoretical result appears to be confirmed by comparison with other independent indications. A new method of locating regions of upwelling with the approximate velocity is proposed.

INTRODUCTION

Since 1949, cruises of the California Cooperative Oceanic Fisheries Investigations off the California coast have provided oceanographic data at close to 100 stations each month, and the main purpose of the present study is to reconsider the problem of upwelling from these data. Upwelling in this area has long been recognized by the presence of conspicuous cold and saline surface water localized in some regions along the coast, and attention has been paid to this striking phenomenon because of its biological importance in relation to the productivity of the area. Various authors (Thorade, 1909; McEwen, 1912, 1929; Sverdrup, 1938; Sverdrup and Fleming, 1941) have discussed the problem from observed distributions of temperature, salinity or some other factors and have attempted to account for it by applying the Ekman theory of wind-driven current to the coastal region.

It appears, however, that existing theory does not account for all of the upwelling which actually takes place off the California coast. From these recent observations, which give certain characteristic features of the distribution of properties indicating certain types of circulation in the regions, somewhat smoothed features of upwelling

[1] This manuscript was prepared at Scripps Institution of Oceanography and was read at the 35th Annual Meeting of The American Geophysical Union at Washington, D. C. in 1954. Except for editorial emendations, only small changes have been made in the original manuscript that was presented in 1954 in Washington.

Since this manuscript was prepared, Stommel (1956) has obtained essentially the same expression for the vertical velocity.

Contributions from the Scripps Institution of Oceanography, New Series, No. 963.

appear to be predictable on a basis of dynamical balance. The mean distribution and seasonal variations in upwelling computed from the data seem to be derived from those of the large-scale wind distribution. Various practical methods of estimating upwelling quantitatively are derived from the theoretical results. At present the most reliable estimate is provided by computation of the subsurface meridional current from the available density distribution in the lower layers. Although results are encouraging when compared with various other independent indications, the validity of our results is probably limited due to various uncertainties involved and to some short-comings in methods. Because of the lack of direct measurement of vertical velocity, which is extremely difficult to determine at present, and because of difficulties in obtaining reliable horizontal divergence from a directly measured horizontal current, critical tests are still lacking. Yet the proposed theory and method seem to apply also to various other parts of the ocean where vertical motion is significant.

THE MODEL

The discussion is based on monthly averages and on one degree rectangles in latitude and longitude; use of such hydrographic observations does not permit treatment in detail, but it does permit greater simplification of the theoretical discussion. Thus our procedure gives results which are significant in an average sense only. For instance, the results will not show upwelling of only a few days' duration or of a few kilometers' extent, nor will they allow for other local disturbances or for internal or surface tides. Also, our estimated velocity will be somewhat smaller in general than the instantaneous.

Let us take the rectangular co-ordinates in which the positive x, y, and z axes point east, north and vertically downward, respectively. By eliminating the horizontal pressure gradient from the original equations of motion, we obtain the approximate vorticity equation

$$(1)\quad D/Dt\,(\zeta + f) = -(\zeta + f)\,div\,\mathbb{V} - (\partial/\partial z)\,\mathrm{curl}_z\,\tau_s + B\nabla_H^2\zeta;$$

here $\mathbb{V}$ denotes the two dimensional (horizontal) velocity vector, with the components u and v in the x and y direction respectively, $f = 2\omega \sin(\varphi)$ is the Coriolis parameter, ω is the earth's angular velocity, φ is latitude, ζ is the vertical component of relative vorticity, τ_s is vertical shearing stress with the components τ_{sx} and τ_{sy} in the x and y direction respectively, and B is the coefficient of lateral mixing.

The relative importance of the order of magnitude in each term should depend largely on the *scale* of the processes with which we are concerned. The following is most essential to our estimate of the order of magnitude on which the whole discussion is based:

We deal with (1) time and space averages of one month and 100 km, (2) middle and low latitudes, (3) comparatively weak currents of about 20 cm/sec, (4) predominantly meridional currents. Now, for convenience, let us assume a model two-layer ocean. The density profile in California waters consists essentially of the upper (mixed) layer, the transitional layer, and the lower layer. The upper layer, which is characterized by a stratum of intense wind stirring and vertical mixing, varies between 10 and 200 m in thickness, a mean thickness of 50 m being assumed in the present estimate. The transitional layer has a greater vertical stability than the other two, and, in practice, it can be disregarded for the present discussion. In the lower layer there is much less stirring and mixing than in the upper layer and its thickness is taken to be 500 m.

The geographic conditions of the area give $f = 0.7 \times 10^{-4}\text{sec}^{-1}$ and $\beta = Df/Dy = 2 \times 10^{-13}\text{sec}^{-1}\text{cm}^{-1}$ approximately. The averaging procedures, as stated, may yield $\partial/\partial t \sim (\text{one month})^{-1} \sim 4 \times 10^{-7}$ sec^{-1}, and $\partial/\partial x$, $\partial/\partial y \sim (100\text{km})^{-1} \sim 1 \times 10^{-7}\text{cm}^{-1}$. Further, we assume the following numerical values: $v \sim 20$ cm/sec and $B \sim 5 \times 10^{7}\text{cm}^{2}\text{sec}^{-1}$ for the upper layer and $v \sim 5$ cm/sec and $B \sim 1 \times 10^{7}$ $\text{cm}^{2}\text{sec}^{-1}$ for the lower layer. The numerical values of these fundamental quantities give the approximate order of magnitude to the estimated values of quantities for each term in the vorticity equation, as shown in Table I. The order of magnitude of dominant terms in the vorticity equation appears to be some 10^{-11}sec^{-2} in the surface layer and 10^{-12} sec^{-2} in the lower layer. This is likely to make it necessary to assume $div \; \mathbb{V} \sim 0(10^{-7})$ in the surface layer and $0(10^{-8})$ in the lower layer. The relative magnitude of the quantities appearing in the vorticity equation, estimated on a basis of combinations of the fundamental quantities, is shown in Table I.

TABLE I.

Term	*Surface Layer*	*Lower Layer*
$\partial\zeta/\partial t$	$0.08 \times 10^{-11}\text{sec}^{-2}$	$0.2 \times 10^{-12}\text{sec}^{-2}$
$u\,\partial\zeta/\partial x + v\,\partial\zeta/\partial y$	$0.4 \times 10^{-11}\text{sec}^{-2}$	$0.25 \times 10^{-12}\text{sec}^{-2}$
$\beta v\ (= Df/Dt)$	$0.4 \times 10^{-11}\text{sec}^{-2}$	$1 \times 10^{-12}\text{sec}^{-2}$
$(\zeta + f)$ div $\mathbb{V}$	$0.9 \times 10^{-11}\text{sec}^{-2}$	$1 \times 10^{-12}\text{sec}^{-2}$
$\dfrac{\partial\ \text{curl}_z}{\partial z}\tau_z$	$0.8 \times 10^{-11}\text{sec}^{-2}$	$0.05 \times 10^{-12}\text{sec}^{-2}$
$B\nabla_H{}^2\zeta$	$0.2 \times 10^{-11}\text{sec}^{-2}$	$0.05 \times 10^{-12}\text{sec}^{-2}$

It is seen that horizontal divergence is one of the most important terms in the vorticity equation which balances stress vorticity in the

surface layer and planetary vorticity in the lower layer. It follows that the vertical velocity near the boundary between these two layers can be found *by knowing either the distribution of surface wind stress or the north-south component of the current in the lower layer.*

According to the values in Table I, the original vorticity equation is simplified into

$$\frac{\partial w}{\partial z} = \frac{\beta}{f} v + \frac{1}{f} \frac{\partial \operatorname{curl}_z \tau_z}{\partial z}, \tag{2}$$

where we used

$$\operatorname{div} \mathbb{V} = -\frac{\partial w}{\partial z}$$

and where w is the vertical component of velocity, v a north component of velocity, and t time.

Retaining terms under corresponding approximations, the equations of motion from which (2) is derived are:

$$-fv = -\frac{\partial p}{\partial x} - \frac{\partial \tau_{zx}}{\partial z} \tag{3}$$

$$+fu = -\frac{\partial p}{\partial y} - \frac{\partial \tau_{zy}}{\partial z},$$

where p is pressure.

Flow at the surface and bottom of the sea is required along the boundary surfaces. Then we find, upon integrating (2), that

$$w|_z = -\frac{\beta}{f^2}\int_z^D \frac{\partial p}{\partial x}\, dz - \frac{1}{f}\operatorname{curl}_z (\tau_D - \tau_z) - \frac{\beta}{f^2}(\tau_{zx}|_0 - \tau_{zx}|_z) + \frac{1}{f}\left\{\left.\frac{\partial p}{\partial x}\right|_D \frac{\partial D}{\partial y} - \left.\frac{\partial p}{\partial y}\right|_D \frac{\partial D}{\partial x}\right\}, \tag{4}$$

where D is the vertical co-ordinate for the sea bottom. This is valid for the whole column, but for the surface layer a more convenient form is given by

$$w|_z = \frac{\beta}{f^2}\int_{z_0}^z \frac{\partial p}{\partial x}\, dz - \frac{\beta}{f^2}\left(\tau_x + \frac{f}{\beta}\operatorname{curl}_z \tau\right) + \frac{\beta}{f^2}\left(\tau_{zx} + \frac{f}{\beta}\operatorname{curl}_z \tau_z\right), \tag{5}$$

where z_0 is the vertical co-ordinate for the sea surface, and τ is the surface wind stress with its components τ_x and τ_y.

Assuming that the effect due to the current near the bottom is negligible and considering that stress vorticity is small in the lower layers (especially in the intermediate layers), vertical velocity at a level $z = H$, where the stability is great, say 150m, is given by

$$(6)^2 \qquad w_H = -\frac{\beta}{f^2}\int_H^D \frac{\partial p}{\partial x}\,dz = -\frac{\beta}{f}\int_H^D v\,dz\,.$$

Equations (5) and (6) represent the vertical component of flow across a horizontal plane.

For $z = h$, where h is the depth of the mixed layer, (5) becomes

$$(7) \qquad w_h = \frac{\beta}{f^2}\int_{z_0}^h \frac{\partial p}{\partial x}\,dz - \frac{\beta}{f^2}\left(\tau_x + \frac{f}{\beta}\,\mathrm{curl}_z\,\tau\right)$$

which can practically be reduced to

$$(8) \qquad w_h \sim -\frac{1}{f}\,\mathrm{curl}_z\,\tau\,.$$

Equation (6) indicates a close relationship between *vertical velocity at $z = H$ and meridional mass transport in the layers below $z = H$.* In both hemispheres, therefore, the subsurface *poleward* component of the current must be associated with ascending motion. In accordance with theory, we may then anticipate the following facts which are confirmed in reality (see later sections): In California waters, ascending motion exists in inshore areas with the northbound current in lower layers while descending motion occurs offshore with the southbound current in lower layers. Although numerical integration of (6) can be performed, the method can be somewhat simplified by making use of the characteristics of density structure in the areas. This practical method will be discussed in the next section, Calculations.

A possible role of planetary vorticity in the horizontal divergence of deep currents was noted by Ekman (1923, 1932), and the remarkable role played by Coriolis change in deriving horizontal divergence and in a mutual adjustment between upper and lower layers has been suggested in studies of large-scale oceanic circulation by Sverdrup (1947), Stommel (1948), Reid (1948), Hidaka (1949), and Munk (1950). On the other hand, eq. (8) indicates that upwelling takes place in the region where the wind stress curl is positive, as in inshore areas off California under usual conditions. Especially in forecasting upwelling, use of meteorological information would be most desirable. Furthermore, since serious errors in oceanographic data could be caused by the presence of internal waves due to stratification of the water, estimation from surface winds certainly would have an advantage. Although some difficulties prevent experimenta-

[2] Note that (6) is valid even if the shearing stress is not negligible at any intermediate depths between H and D.

tion in this direction, it would be worthwhile if the general features of vertical circulation and their variations, seasonal or yearly, could be related to the features and variations in a field of wind stress curl and to those in the North Pacific anticyclonic system as well. Climatological conditions in the eastern North Pacific will be principally responsible for causing quasi-steady variations in vertical transport of water in inshore areas off California.

Roughly speaking, the horizontal divergence introduced and maintained by surface winds is compensated by horizontal convergence in subsurface layers produced by poleward transport of water, thus leading to the upward transport of water from lower layers into the surface layer. However, "upwelling" in a real sense should refer to the ascent of water from lower layers *into* the surface layer, even *up to* the very surface. However, the discussion of this phenomenon cannot be accomplished at present, mainly due to lack of knowledge of surface distributions of turbulence.

Attention should also be paid to the fact that the mechanism of upwelling considered above is more or less free from the direct influence of boundary conditions at the coast. This is essentially different from the interpretation of the boundary phenomenon in coastal upwelling. The latter should account for a phenomenon more localized in space as well as in time (Yoshida, 1955a, 1955b). The effects of bottom topography are only partially included in our considerations, since density distributions are considerably influenced by them. Our computations are limited to areas where depths exceed 1000m, with areas close to the coasts excluded. The detailed structure of vertical circulation in the California areas might therefore reveal many local and temporary features which have escaped us.

CALCULATIONS

This section is concerned with a practical method of simplification to obtain the numerical values for the integral (6), where certain approximations may be permissible. The method, however, appears to be quite useful in avoiding complicated computations and of reducing the number of required observations.

If we denote

$$P_H = \int_H^D p \, dz, \tag{9}$$

where D and H are assumed constant, it is seen that

$$w_H = -\frac{\beta}{f^2}\frac{\partial P_H}{\partial x} = \frac{g\beta}{f^2}\int_H^D (z - H)\frac{\partial \rho}{\partial x}\, dz \tag{10}$$

provided that a hydrostatic pressure is assumed and that the pressure gradient is considered negligible below a level $z = D$. Of course, (10) can be integrated numerically without difficulty if we have enough observed values for ρ and if we assume a reference level, say $D = 1000$m. However, it would be convenient if we could avoid the numerical integration by making use of the characteristic density structure in California waters. The vertical distributions of density show certain regularities so that a few parameters may be sufficient to characterize the structure. Now an attempt is made to evaluate $\partial P_H/\partial x$ in terms of those parameters which can be measured. The density profile consists essentially of three layers, as stated before; of these the transitional layer has a greater stability than the other layers, and in most cases a level of *150*m falls within this layer, mostly in the center. Comparison clearly indicates that $P(H)$ and consequently $w(H)$ can be determined practically by the *density structure in the lowest layer only.* Both results consistently imply that $P(H)$ and its derivatives can be determined, with good approximation, by a *density at a level between 600 to 1000m, probably 700 to 800m.* Vertical velocity can then be determined by (10), for $H = 150$m:

$$w_H = \frac{0.39 \times 10^{-2}}{\tan \varphi \sin \varphi} \nabla_x \sigma_7 \,, \tag{11}$$

where ∇_x denotes a difference in σ_7 over 100km distance (east value minus west value) and σ_7 is σ_t at a 700m level. Putting

$$w_H = U(\varphi)\, \nabla_x \sigma_7 \quad , \tag{12}$$

the values of $U(\varphi)$ for various latitudes can be tabulated as follows:

φ :	25°	30°	35°	40°	45°
$U(\varphi)$: $10^{-2}x$	1.95	1.34	0.98	0.72	0.55

This will give 0.7×10^{-3}cm/sec or 16m/month as the value of w for $\nabla_x \sigma_7 = 0.05$ and $\varphi = 30°$.

One of the uncertainties involved in this estimation of w is the pressure gradient at greater depths. This difficulty can hardly be avoided since the method is based entirely on a divergence of horizontal currents which are based on measurements of dynamic topography relative to a deep layer. One may speculate that the presence of the pressure gradient at greater depths should largely depend upon the degree of departure from the equilibrium state. Hence the above argument should depend on the scale of period or area over which vertical velocity is averaged. The considerable pressure gradient which is present at greater depths at the initial stage of surface con-

dition changes will possibly disappear as the mass-adjustment goes on. In the present computations, then, it is assumed tentatively that the effect of the pressure gradient below the 1000m level is negligible. We have prepared charts indicating the horizontal distributions of w_H from data taken on each CCOFI cruise (made almost every month) during 1949 and 1950. All of the numerical values of w are based on eq. (12), although we employed σ_t at the 800m level instead of at 700m.

COMPARISON WITH OTHER OBSERVATIONS

In addition to such indications of upwelling as more or less localized surface water of low temperature, high salinity and low oxygen content, there may be other phenomena which are likely to indicate upwelling or sinking. The following descriptions give certain observed indications of upwelling in the areas concerned. (1) *Increase in density at the 150m level from month to month compared to estimated upwelling.* In general, if upwelling takes place, isopycnals would be expected to rise in the upper layers. Charts (Figs. 1, 2) indicating local time changes in σ_t at the 150m level which are found from month to month and season to season are compared with distribution charts of w_H which are obtained from our method. In almost all cases the results agree surprisingly well considering that some of the σ_t changes would be due to horizontal motion or to the effect of internal waves.

(2) *Changes in Oxygen and Phosphate in the Surface Layer.* Examples have been obtained for which changes in O_2 and PO_4-P at levels above 150m occur just as predicted by our estimation of vertical motion at 150m.

(3) *High Density Regions and High Density Tongues in the Surface Layer.* Although the estimated w_H indicates only the *vertical component* of flow at the 150m level, regions of ascending motion agree satisfactorily with those of high surface density (averaged density for surface layer), especially in areas of very high density. In vertical sections where upwelling is indicated, in most cases from conspicuous high surface density, the density in layers between 600 and 1000m is found to decrease toward the coast.

(4) *Seasonal Variations and their Relation to those in the Wind Field.* Distributions of estimated ascending motion show more or less continuous variations from season to season, although the variations do not appear to be as simple as those that have been considered (Sverdrup, *et al.*, 1942). Joseph L. Reid, Jr., of Scripps Institution of Oceanography (personal communication) has computed time changes in temperature, salinity and oxygen between cruises and has found that

Figure 1. Changes in density (σ_t from observations) at the 150m level from April to June 1949.

upwelling occurs more frequently during the year and at more places along the coast than had been previously suggested.

Satisfactory agreement is found in a comparison of charts of seasonal averages of w_H and density changes at the 150m level during seasons. Vertical sections along the coasts for stations nearest to the coasts for

Figure 2. Computed vertical velocity (w_H) at the 150m level for May 1949.

1949 and 1950 show numerous cases of a conspicuous rise of isopycnals which are likely to indicate upwelling. Note that inshore areas south of Point Conception show no upwelling during the period between June and September whereas those north of Point Conception do. The three illustrations in Fig. 3 give typical examples. At St. 1201, south of Point Conception, upwelling occurs in spring. At St. 801,

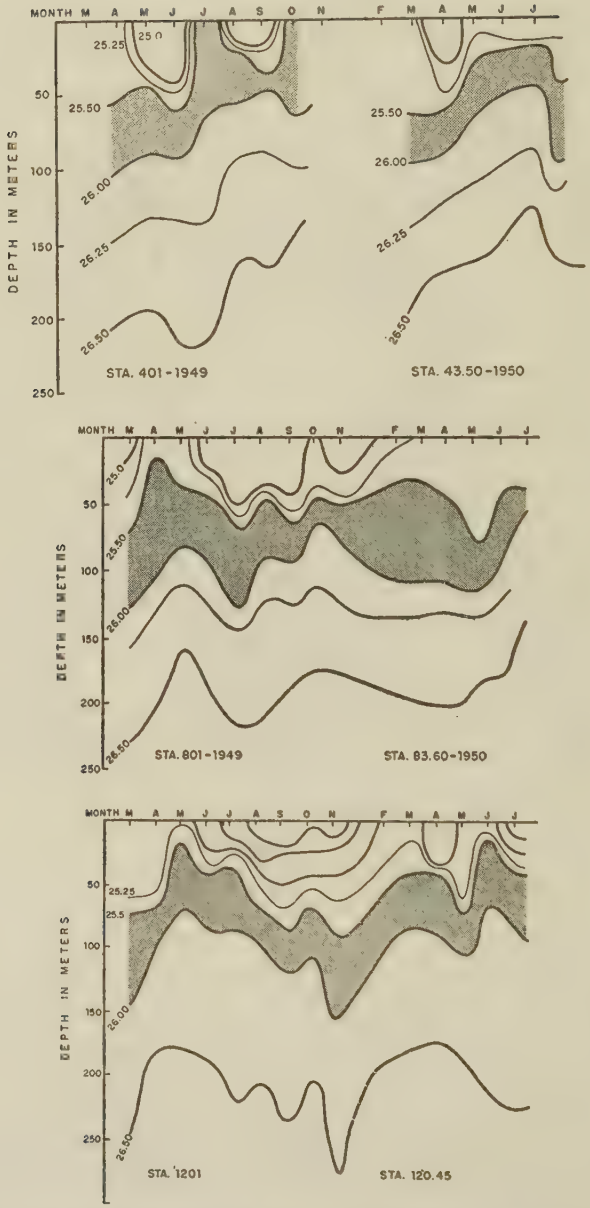

Figure 3. Monthly changes in vertical density distribution (σ_t) at three positions off the California coast.

near Point Conception, it occurs twice during the year, in spring and in fall. At St. 401, north of Point Conception, upwelling is indicated during summer and fall. An offshore station (909), a southern inshore station (902) and a northern inshore station (502) provide typical examples of estimated vertical velocity. From our estimates as well as other indications, intensive upwelling occurs only during spring in southern inshore areas and only during summer and fall in northern inshore areas.

These characteristics are accounted for mainly by *surface wind curl.* Charts prepared by us of the distribution of wind curl over California waters, computed from statistical wind data based on 5° squares of latitude and longitude in 1949–50, show that the boundary where curl $\tau = 0$ is located somewhat parallel to the coastline, approximately 500 km offshore, with positive curl inshore. The most typical contrast in winds is found as follows: (1) during spring, March to May, southern inshore regions show curl $\tau > 0$ while northern inshore regions show curl $\tau < 0$; (2) conversely, during summer, June to August, curl $\tau > 0$ is found in northern inshore regions while curl $\tau < 0$ is found in southern inshore areas. Thus characteristic seasonal variations in upwelling appear to correspond to wind curl variations.

APPLICABILITY OF OUR METHOD TO OTHER AREAS OF THE OCEAN

Since our method is based on the subsurface vorticity balance (latitudinal effect), it will be valid in *middle and low latitudes* and especially in areas where *meridional currents prevail in lower layers.* Regions off the western coasts of continents, as off California, Peru, and western Africa, will be typical upwelling areas belonging in the same category; also, the western boundaries of the oceans where the Kuroshio and Gulf Stream occur may be included.

On the other hand, the surface vorticity balance (wind effect) appears to be applicable for wide areas of the oceans; however, an exception may be found in the western boundary of the oceans, where the numerical value of the wind stress curl may be small in comparison with lateral stress curl, nonlinear relative vorticity or planetary vorticity owing to narrow intensified currents. Over large areas of the central oceans (in the northern hemisphere), statistical wind distributions indicate the area of negative wind stress curl which nearly covers the latitudes between 15° and 50° N, corresponding to the areas associated with the subtropical anticyclonic wind system. The descending flow over such an area, corresponding to the Subtropical Convergence, has been reported by various authors.

Off the Peruvian coast, Gunther (1936) found that the subsurface countercurrent flows south (poleward) close to the coasts and that surface *anticyclonic* swirls (southern hemisphere) develop where upwelling is found. Similar subsurface poleward currents close to the coasts are indicated along the western coasts of North Africa and of South Africa where upwelling has been reported (Defant, 1936). The wind stress curl theory has been applied to the vertical motion in the Gulf Stream by Neumann (1952) and the planetary vorticity theory has been discussed by Hansen (1952).

CONCLUSIONS

Although the rule derived for estimating upwelling appears to be valid, one should remember the uncertainties involved, among which the following are important: (1) Features which are local or temporary are excluded in our estimated gross features. (2) Pressure gradient or current at deep layers may modify our result to a considerable extent in spite of the small magnitude. (3) "Upwelling," meaning upward penetration of a mass of water into a surface mixed layer, cannot be fully discussed owing to our incomplete knowledge of the effects of turbulence. (4) Values of density at each station obtained from one hydrographic cast *may not* represent the monthly mean but may be effected by irregular or temporary disturbance at the time of observation or by periodic fluctuation due to *internal waves*. (5) Errors may be introduced in using a single-level-density method since its validity may fail if significantly different types of stratification of water masses are encountered.

In spite of these uncertainties, remarkable agreement is found between the predicted upwelling and other independent indications of upwelling. Some of the agreement is so encouraging that we are inclined to believe the reality of the estimated results and of the method.

The major features of vertical motion in California waters as derived in this paper are confirmed by comparison with other methods. The principal mechanism involved in our considerations is that surface horizontal divergence caused by wind stress is compensated by subsurface convergence associated with subsurface poleward transport due to the poleward increase in Coriolis parameter. The magnitude of this upward velocity, at the thermocline layer, can roughly account for the surface upwelling velocity which is induced by surface wind stress curl and which causes the changes in observed surface density. It is fairly well established that the larger-scale meteorological conditions are primarily responsible for upwelling and its variations in the California coastal region. Hindcasting of upwelling is found possible from the available oceanographic data and from surface wind curl.

Various methods for deriving vertical velocity are suggested, the most reliable of which would be that given by computations of meridional transport over the layers underlying a certain level, say 150 m. Although a simplified method is employed for the present computations by using density distributions at the 700 or 800 m level, the computations of subsurface meridional transport by means of pressure computations should find more general applicability in the large part of the open ocean in middle latitudes as well as in the eastern and western boundaries of the ocean where meridional currents are dominant due to the coastal barriers. The relation between wind stress curl and upwelling will be valid more widely, with the probable exception for the western boundary of the oceans.

ACKNOWLEDGEMENT

The authors wish to express their appreciation to Dr. Walter H. Munk and Dr. Robert S. Arthur for discussions and encouragement; to Mr. Joseph L. Reid, Jr. for discussions and consideration of the manuscript; to Mr. Hans T. Klein for assistance in the preparation of the manuscript; to Dr. Gordon W. Groves and Dr. Charles S. Cox for helpful advice and suggestions and also for editorial assistance.

REFERENCES

Defant, A.

1936. Das Kaltwasserauftriebsgebiet vor der Küste Südwestafrikas. Länderkundliche Forschung, Festschrift Norbert Krebs zur Vollendung 60, Lebensjahres dargebracht, pp. 52–66.

Ekman, V. W.

1923. Über Horizontalzirkulation bei winderzeugten Meeresströmungen. Ark. Mat. Astr. Fys., *17* (26), 74 pp.

1932. Studien zur Dynamik der Meeresströmungen. (Gerlands) Beitr. Geophys., *36:* 385–438.

Gunther, E. R.

1936. A report on oceanographical investigations in the Peru Coastal Current. 'Discovery' Rep., *13:* 107–276.

Hansen, Walter

1952. Einige Bemerkungen zum Golfstromproblem. Dtsch. hydrogr. Zeit., *4:* 80–94.

Hidaka, Koji

1949. Mass transport in ocean currents and lateral mixing. Geophys. Notes, Tokyo, *2* (3): 1–4.

McEwen, G. F.

1912. The distribution of ocean temperatures along the west coast of North America deduced from Ekman's theory of the upwelling of cold water from the adjacent ocean depths. Int. Rev. Hydrobiol., *5:* 243–286.

1929. A mathematical theory of the vertical distribution of temperature and salinity in water under the action of radiation, conduction, evaporation, and mixing due to the resulting convection. Bull. Scripps Inst. Oceanogr., *2:* 197–306.

MUNK, W. H.

1950. On the wind-driven ocean circulation. J. Meteorol., *7* (2): 79–93.

NEUMANN, GERHARD

1952. Some problems concerning the dynamics of the Gulf Stream. Trans. N. Y. Acad. Sci., (II) *14* (7): 283–291.

REID, R. O.

1948. The Equatorial currents of the eastern Pacific as maintained by the stress of the wind. J. mar. Res., *7:* 74–93.

STOMMEL, HENRY

1948. The westward intensification of wind-driven ocean currents. Trans. Amer. geophys. Un., *29:* 202–206.

1956. On the determination of the depth of no meridional motion. Deep-Sea Res., *3* (4): 273–278.

SVERDRUP, H. U.

1938. On the process of upwelling. J. mar. Res., *1* (2): 155–164.

1947. Wind-driven currents in a baroclinic ocean; with application to the equatorial currents of the eastern Pacific. Proc. nat. Acad. Sci., *33:* 318–326.

SVERDRUP, H. U. AND R. H. FLEMING

1941. The waters off the coast of Southern California, March to July, 1937. Bull. Scripps Inst. Oceanogr., *4* (10): 261–378.

SVERDRUP, H. U., M. W. JOHNSON AND R. H. FLEMING

1942. The Oceans. Prentice Hall, Inc., New York. 1087 pp.

THORADE, H.

1909. Über die Kalifornische Meerestromunge. Ann. Hydrogr., Berl., *37:* 17–34. 63–76.

YOSHIDA, KOZO

1955a. Coastal upwelling off the California coast. Rec. Oceanogr. Works Japan *2* (2): 8–20.

1955b. An example of variations in oceanic circulation in response to the variations in wind field. J. oceanogr. Soc. Japan, *11* (3): 103–108.

AN EXTERNAL CORE CATCHER FOR OCEANOGRAPHIC WORK

By

WILLIAM H. GLEZEN

Gulf Research and Development Company, Houston, Texas

ABSTRACT

A core catcher for use with short gravity-type core barrels is described. A flat plate at the foot of a pair of pivot arms is caused to swing under the bottom of the core barrel after the barrel is withdrawn from the bottom. A float-weight lever arm is employed to actuate the device.

INTRODUCTION

In a program requiring the collection of about 200 pairs of small cores for foraminiferal studies, the Phleger Bottom Sampler[1] was selected as a sampling device. Two 75-pound lead blocks were clamped to the 50-pound core barrel, and the resultant 20-pound corer penetrated several inches into clean well-sorted sands. The bearing surface at the base of the lead weights was usually sufficient to prevent excessive penetration into soft muds.

Samples were collected from water depths of 200 to 600 feet and in sediments ranging from soft clayey muds to clean, well-sorted, fine to medium-grained quartz sands. Several samples contained or consisted entirely of calcareous particles ranging in size from 0.5 to 10 mm.

In the initial phase of collecting considerable difficulty was encountered in retaining cores in the core barrel while raising the instrument to the surface. In spite of various modifications of the ball valve and the use of spring leaf core catchers, repeated lowerings were frequently required to recover a core, and in some cases even repeated effort failed.

Spring leaf core catchers have the following operational shortcomings: (1) The spring fingers gouge the core as it enters the barrel through the cutting head; (2) the catcher frequently fails to close after jamming on coarse particles; (3) the catcher fails to retain fine, well-sorted sands that wash out or turn into quicksand and flow out through small openings between the leaves.

[1] Phleger, F. B., Ecology of Foraminifera, Northwest Gulf of Mexico, Mem. Geol. Soc. Amer., 46, Pt 1: 3.

The action of the ball check valve commonly used in the top of the Phleger Bottom Sampler retains a mud core satisfactorily when samples are taken in shallow water. However, in water deeper than about 40 feet, a defect in the check valve may permit even a mud core to escape while the core barrel is being raised to the deck.

Failure to recover a short core may represent a substantial loss in limited and expensive marine-sampling time, and such difficulty may prevent coring of entire areas. Therefore the construction and adjustment of an efficient core catcher is justified. The core catcher described below has been specifically designed for use on the continental shelf where a wide range of sediment types are encountered in water depths of 40 to 600 feet.

DESCRIPTION OF THE CORE CATCHER

The core catcher developed is a flat plate swinging on two arms which pivot from the weight holder of the core barrel. The plate is held clear of the barrel while it is being lowered to the sea floor and swings under the barrel when it is raised through the water. A lever arm with a weight at one end and a float at the other extends across the plate and controls its position in the water.

In air, before striking the water, the core catcher is held by a hook which swings free when the core barrel enters the water. While the barrel is being lowered through the water, the float supports the core catcher and counterbalances the lead weight which has a short effective lever arm in this position. When the core barrel is raised, the water resistance of the float drags the core catcher down, progressively decreasing the effective lever arm of the float and increasing the effective lever arm of the lead weight; thus the weight-float balance is reversed. The lead weight swings the core catcher down until the plate slides under the bottom of the core barrel and is locked into position by the gravity latch (Fig. 1).

After a core catcher of similar dimensions to the one shown (Fig. 2) has been constructed, the balance required can be obtained by trial and error. Adjustment of the lead weight and of the position of a stop, limiting the upward swing of the core catcher, will permit the core catcher to balance properly.

The float, sold commercially for use on fish nets, is made of hollow plastic 5 inches in diameter by $8\frac{3}{4}$ inches long with a displacement of 138 cubic inches and a buoyancy of 5 pounds. Any sturdy float of this type should be satisfactory. Two may be required if the core catcher is somewhat heavier than the original.

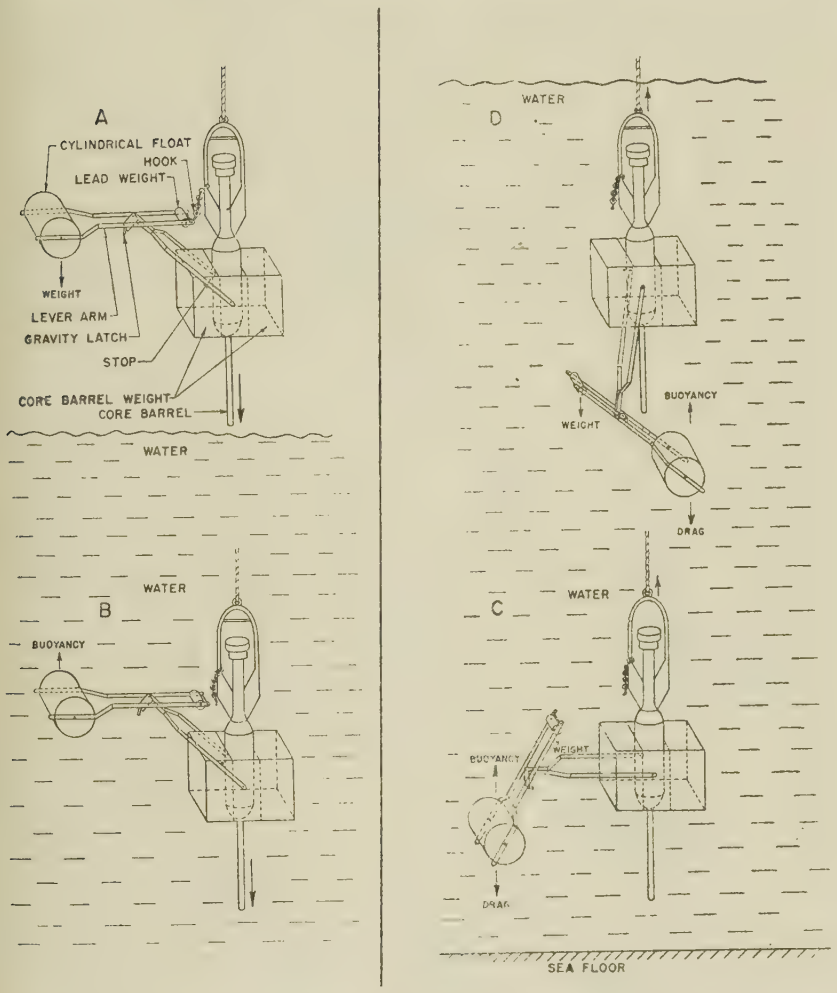

FIGURE 1. Core catcher mounted on Phleger bottom sampler: (A) in cocked position before lowering; (B) floating in up position during lowering; (C) swinging down while corer is raised from the sea floor; (D) closing of core catcher by combined effect of float & weight.

In its present form this device is limited to core barrels less than two feet long. It is believed that this type of core catcher could be adapted for use with long piston-type core barrels by mounting it on a sliding carriage. The carriage could be released from the top of the core

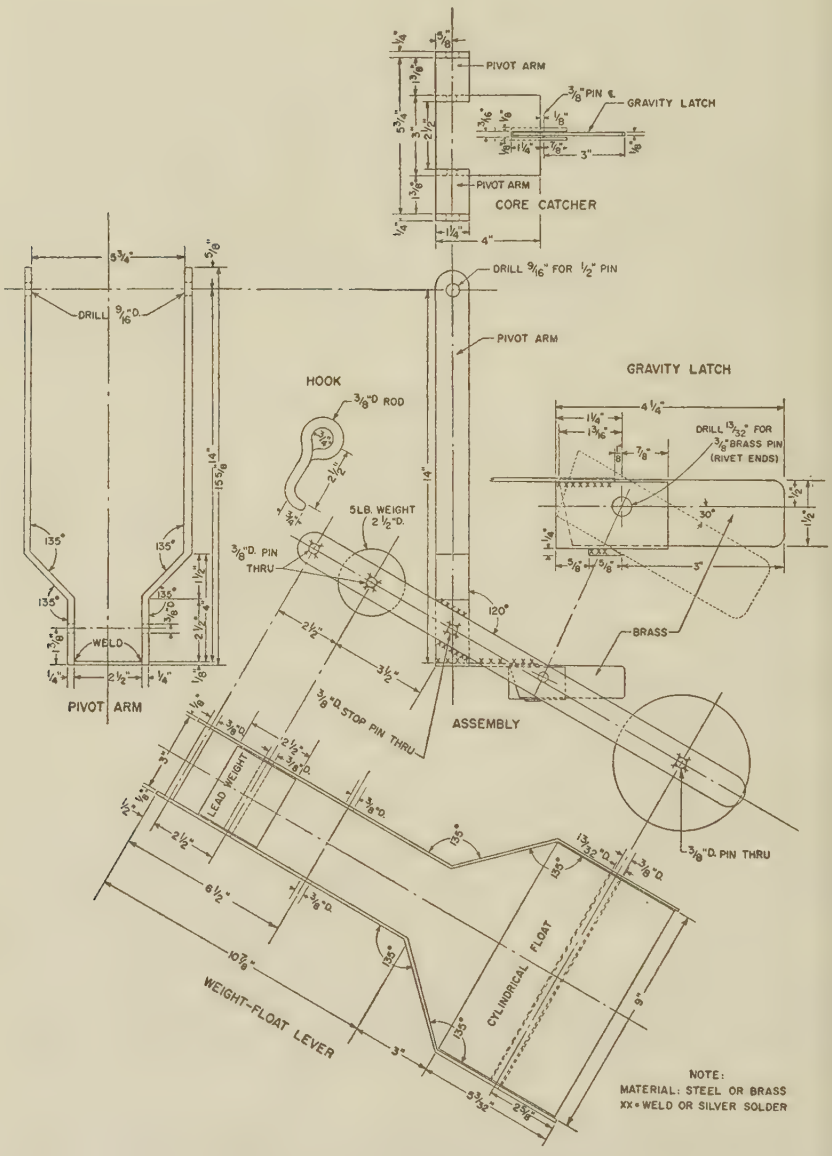

FIGURE 2. Plans for external core catcher.

barrel when it is raised through the water so that it could slide freely down the barrel and strike the cutting head. The core catcher would then swing into position as before.

ACKNOWLEDGMENTS

The author wishes to thank Dr. R. B. Wescott, Executive Vice President, Gulf Research & Development Company, for permission to release the information contained in this paper. The author is grateful for the editorial assistance of Dr. J. C. Ludwick in the preparation of this paper.